Action Potential Modulates Ca^{2+}-Dependent and Ca^{2+}-Independent Secretion in a Sensory Neuron

Hui Zheng,[†] Juan Fan,[†‡] Wei Xiong,[†] Chen Zhang,[†] Xiao-Bing Wang,[†] Tao Liu,[†] Hong-Ju Liu,[†] Lei Sun,[†] Ye-Shi Wang,[†] Liang-Hong Zheng,[†] Bai-Ren Wang,[‡] Claire Xi Zhang,[†*] and Zhuan Zhou[†§*]

[†]Institute of Molecular Medicine, Peking University, Beijing, China; [‡]Institute of Neurosciences, the Fourth Military Medical University, Xi'an, China; and [§]State Key Laboratory of Biomembrane Engineering, Peking University, Beijing, China

ABSTRACT Neurotransmitter release normally requires calcium triggering. However, the somata of dorsal root ganglion (DRG) neurons possess a calcium-independent but voltage-dependent secretion (CIVDS) in addition to the classic calcium-dependent secretion (CDS). Here, we investigated the physiological role of CIVDS and the contributions of CIVDS and CDS induced by action potentials (APs) in DRG soma. Using membrane capacitance measurements, caged calcium photolysis, and membrane capacitance kinetics analysis, we demonstrated that AP-induced secretion had both CIVDS and CDS components. Following physiological stimuli, the dominant component of AP-induced secretion was either CIVDS for spontaneous firing or CDS for high-intensity stimuli. AP frequency modulates CDS-coupled exocytosis and CIVDS-coupled endocytosis but not CIVDS-coupled exocytosis and CDS-coupled endocytosis. Finally, CIVDS did not contribute to excitatory postsynaptic currents induced by APs in DRG presynaptic terminals in the spinal cord. Thus, CIVDS is probably an essential physiological component of AP-induced secretion in the soma. These findings bring novel insights into primary sensory processes in DRG neurons.

INTRODUCTION

In neurons and neuroendocrine cells, transmitters and peptides released from secretory vesicles play key roles in neural signal transduction (including sensing pain), synaptic plasticity, and learning and memory. Vesicle release is generally initiated by action potentials (APs) depolarizing the plasma membrane. Voltage-dependent Ca^{2+} channels then open for Ca^{2+} influx, followed by the fusion of vesicles with the plasma membrane and subsequent transmitter release. This fusion event is believed to be strictly regulated by Ca^{2+} (1,2) and has been confirmed in many cell types, such as the neuromuscular junction, central nerve terminals, and adrenal chromaffin cells (3–7). In these models, depolarization fails to induce secretion in the absence of extracellular Ca^{2+}. However, whether voltage per se also affects secretion remains controversial. For example, some voltage sensors, such as the L-type and N-type Ca^{2+} channels, are physically linked to the vesicle release machinery (8–16), and therefore, membrane depolarization alone may directly trigger vesicle release.

We previously demonstrated that Ca^{2+}-independent but voltage-dependent secretion (CIVDS) occurs in the somata of DRG neurons (17,18). CIVDS was revealed by a series of independent approaches, such as membrane capacitance measurements, electrochemical carbon fiber electrode recording, and confocal imaging of FM fluorescence. In the absence of extracellular Ca^{2+}, the amplitude of membrane capacitance change is dependent on both voltage and pulse duration. CIVDS is triggered when membrane potential is >-30 mV and reaches a maximum above 0 mV. When the pulse duration reaches 200 ms, the membrane capacitance (C_m) signal also plateaus, suggesting that the CIVDS pools are saturable (19). Furthermore, CIVDS is tightly coupled to a rapid endocytosis (CIVDS-RE) (17). CIVDS-RE is independent of Ca^{2+} and dynamin but is enhanced by increased AP frequency.

The importance of soma secretion has been suggested not only in immune cells, glia cells (20), and endocrine cells (21,22) but also in neurons (23,24). Recently, we demonstrated that an essential functional role of transmitter release from somata is to inhibit high-level activity evoked in locus coeruleus neurons in rat brain slices (25). Following membrane depolarization, somata of DRG neurons release active compounds including CGRP, SP (7,18,26), and ATP (27). This suggests that the somatic secretion may contribute to the function of DRG neurons, including passing primary sensory information and pain sensation. One outstanding question is the physiological function of CIVDS in the somata of DRG neurons.

In this report, we focus on the fractional contributions of CIVDS and CDS to total secretion following physiological AP stimulations. C_m measurements were used to monitor the somatic secretion in DRG neurons while prerecorded real AP waveforms were used as stimuli. We discovered that CIVDS was the prominent form of secretion at low AP numbers and frequencies. CDS and CIVDS-rapid endocytosis (RE), but not CIVDS and CDS-slow endocytosis (SE), were modulated by AP frequency. Finally, CIVDS occurred in the soma and did not contribute to the DRG terminal-induced EPSCs in dorsal horn neuron.

Submitted May 17, 2008, and accepted for publication November 17, 2008.

Hui Zheng and Juan Fan contributed equally to this work.

*Correspondence: zzhou@pku.edu.cn or clairexz@pku.edu.cn

Editor: Robert Hsiu-Ping Chow.

0006-3495/09/03/2449/8 $2.00

doi: 10.1016/j.bpj.2008.11.037

MATERIALS AND METHODS

Isolation of neurons and spinal cord slice preparation

The animal protocols used in this study were approved by the Laboratory Animal Ethics Committee of Peking University. Freshly isolated DRG neurons were obtained as described previously (17) and were used 1–8 h after preparation. Briefly, DRGs were dissected from 100- to 150-g Wistar rats and digested with trypsin (Sigma Chemicals, St. Louis, MO; 0.3 mg/mL) and collagenase (Sigma Chemicals; 1 mg/mL) for 40 min at 37°C. We chose only small neurons (15–25 μm, C-type neurons) with few processes.

Primary dorsal horn (DH)-DRG cocultures were obtained as previously described (28). In brief, DH neurons were isolated from rat embryos aged E13–15, exposed to 0.125% trypsin for 20 min, and dissociated. Similarly, DRGs from the same embryos were isolated separately and exposed to 0.25% trypsin for 25 min and dissociated. DH and DRG neurons were plated on glass coverslips pretreated with poly-L-lysine, and fed with MEM-F-12 and 10% FBS. One day later, the medium was replaced with Neurobasal-B27 and used after at least 6 days.

Transverse spinal cord slices were prepared from segments L1–S3 of 14-day-old rats (29,30). The spinal cord slice with the dorsal root attached was placed in preoxygenated artificial cerebrospinal fluid (ACSF, in mM: 124 NaCl, 2.5 KCl, 2.4 $CaCl_2$, 1.3 $MgSO_4$, 25 $NaHCO_3$, 1.24 NaH_2PO_4, 10 glucose, bubbled with 95% O_2/5% CO_2, pH 7.4) at 1–3°C. After mounting on a vibratome (Vibratome 1000, St. Louis, MO), a 400-μm-thick transverse slice was cut with an attached dorsal root 5–10 mm long. The slice was incubated for at least 1 h in ACSF at room temperature before use, when it was placed on a nylon grid in a slice chamber and superfused (10 mL/min) with ACSF during electrophysiological recording.

Solutions

The standard extracellular solution (pH 7.4) contained (in mM): 150 NaCl, 5 KCl, 2.5 $CaCl_2$, 1 $MgCl_2$, 10 HEPES, and 10 glucose. Ca^{2+}-free solution was the same except that $CaCl_2$ was removed and 1 mM EGTA was added. The intracellular pipette solution (pH 7.2) contained (in mM): 153 CsCl, 1 $MgCl_2$, 10 HEPES, and 4 ATP. For flash photolysis experiments, the intracellular pipette solution (pH 7.2) contained (in mM): 110 Cs-glutamate, 5 NP-EGTA, 8 NaCl, 2.5 $CaCl_2$, 2 Mg-ATP, 0.3 GTP, 0.2 fura-6F, and 35 HEPES. Basal $[Ca^{2+}]_i$ was measured and adjusted to ~300 nM with fura-6F. For Ca^{2+}-imaging experiments, 0.1 mM fura-2 was added to the standard intracellular solution. All chemicals were purchased from Sigma (St. Louis, MO), except for NP-EGTA, fura-2, and fura-6F (Molecular Probes, Eugene, OR).

For spinal cord recording, the extracellular solution was ACSF bubbled with 95% O_2/5% CO_2, and the Ca^{2+}-free extracellular solution for CIVDS recordings was the same except that $CaCl_2$ was removed and 1 mM EGTA and 200 μM Cd^{2+} were added. The intracellular pipette solution (pH 7.2) contained (in mM): 135 K-gluconate, 5 KCl, 0.5 $CaCl_2$, 10 HEPES, and 4 Mg-ATP.

A perfusion system (RCP-2B, INBIO, Wuhan, China) with a fast exchange time (<100 ms) for electronic switching among seven channels was used to change the external medium (31).

Electrophysiological recordings and membrane capacitance measurements

Whole-cell recordings from cultured neurons or spinal cord slices were made using an EPC10/2 amplifier with Pulse software (HEKA Elektronik, Lambrecht/Pfalz, Germany). Cells were voltage-clamped at −70 mV using patch pipettes of 2–4 MΩ. Data were analyzed with Igor software (WaveMetrics, Lake Oswego, OR). Cell C_m was calculated by the "Sine DC" feature of the Pulse lock-in module. A 1 kHz, 20 mV peak-to-peak sinusoid was applied around a DC holding potential of −70 mV. We also used prerecorded real AP waveforms as stimulus templates under voltage clamp as described previously (32). Data were analyzed using Igor software (WaveMetrics).

The superficial laminae of the spinal cord slices were identified under a 4× objective, and individual DH neurons were identified with a water-immersion (40×) objective on an IR-DIC microscope (25). EPSCs or excitatory postsynaptic potentials (EPSPs) from DH neurons were evoked by stimulating the dorsal root with a constant-current pulse through a suction electrode (30). EPSCs were recorded by whole-cell recording from DH neurons under voltage clamp. EPSPs were recorded as field potentials by patch pipettes filled with ACSF.

In primary DH-DRG cocultures, DH neurons were identified by their smaller size and spindle shape (28). EPSCs from DH neurons were recorded by puffing 50 mM KCl onto a nearby DRG neuron.

All experiments were carried out at room temperature (22–25°C), and data are presented as mean ± SE. Significance of differences was calculated using Student's t-test followed by post hoc tests (*$p < 0.05$, **$p < 0.01$, ***$p < 0.001$).

Flash photolysis of caged Ca^{2+} and $[Ca^{2+}]_i$ measurements

For measurement of $[Ca^{2+}]_i$ we used a monochromator-based system (TILL Photonics, Planegg, Germany). The Ca^{2+} indicator fura-6F/fura-2 was excited at 1 Hz with 5-ms light pulses at 340 and 380 nm. The excitation intensity was kept far below the level where photolysis of nitrophenyl (NP)-EGTA occurs. The emission signal was acquired with the fura extension of the Pulse software (Heka Elektronik, Lambrecht, Germany) and sampled by an EPC10/2 amplifier. UV light from a xenon arc flash lamp (Gert Rapp Optoelektronik, Hamburg, Germany) was used to uncage the NP-EGTA, and was coupled with the excitation light into the epifluorescence port of an IX-71 microscope (Olympus, Tokyo, Japan). For all experiments we used an Olympus Uapo/340 40×, 1.35 NA oil immersion objective. Calibration for caged Ca^{2+} experiments followed published methods (33,34). The first flash in each experiment was triggered 2–3 min after the whole-cell configuration was established, allowing recovery of $[Ca^{2+}]_i$ to ~300 nM after the loading transient. $[Ca^{2+}]_i$ was calculated from ratio R of the fluorescent signals at 340 nm and 380 nm with following equation:

$$\left[Ca^{2+}\right]_i = k_{eff}(R - R_{min})/(R_{max} - R).$$

RESULTS

Contributions of CIVDS and CDS to evoked secretion in DRG neurons

To investigate the relative contributions of CIVDS and CDS, we designed experiments to trigger CIVDS, CDS, or both in somata of DRG neurons. To compare pure CIVDS and CDS in the same neuron, we dialyzed the neuron with NP-EGTA-caged Ca^{2+} and Ca^{2+} indicator fura-6F. Somatic CIVDS (C_{m0}) was first induced by a step depolarization from −70 to 0 mV (200 ms) in the absence of a $[Ca^{2+}]_i$ rise (Fig. 1 *A*, *left*; also see Zhang and Zhou (18)). After 2 min, four UV flashes were fired at 0.5 Hz to photorelease the caged Ca^{2+} and increase the $[Ca^{2+}]_i$ level, which resulted in a C_m increase (C_m(UV)) representing an evoked somatic exocytosis. Because no voltage change was involved, C_m(UV) was purely Ca^{2+}-dependent. The series conductance (G_s) and membrane current (I_m) (Fig. 1 *A, lower panels*) were used to monitor the seal condition. The small currents occurring during photorelease may have been caused by a flash

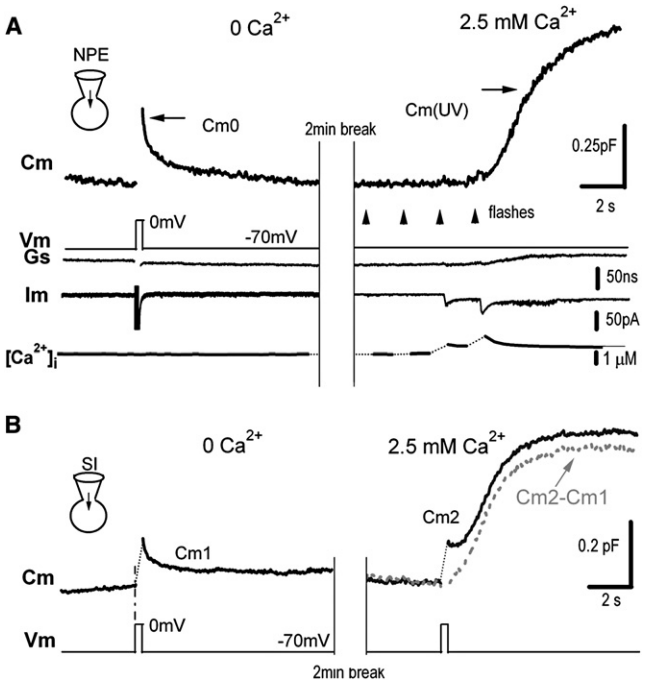

FIGURE 1 Stimulus-induced secretion consists of CIVDS and CDS components in the somata of DRG neurons. (*A*) Depolarization- and UV-flash-induced C_m signals in a DRG neuron dialyzed with 5 mM NP-EGTA and 0.2 mM fura-6F. In Ca2+-free extracellular solution (*left panel*), a step depolarization (200 ms) evoked CIVDS (C_{m0}). When extracellular Ca^{2+} was added (*right panel*), UV flashes (*arrows*) evoked a substantial increase of C_m (C_m(UV)), which was caused by the Ca^{2+} increase in the absence of membrane depolarization. Series conductance (*Gs*) and membrane current (I_m), and Ca^{2+} trace ([Ca^{2+}]i) are also shown. (*B*) Depolarization-induced C_m signals. In Ca^{2+}-free extracellular solution (*left panel*), a step depolarization (200 ms) evoked a C_m increase (CIVDS) followed by a rapid reversal as in *A*. C_{m1} refers to the entire course. Subsequently, extracellular Ca^{2+} (2.5 mM) was puffed (*right panel*), and the same stimulus evoked a biphasic response (C_{m2}). The first Cm increase was followed by a small but rapid reversal and then a slow but substantial increase. $C_{m2} - C_{m1}$ (*dashed line*) indicated the CDS component.

artifact and did not affect C_m measurement (because they did not match the C_m changes).

To determine whether depolarization induces both CIVDS and CDS under normal conditions (in the presence of 2.5 mM external Ca^{2+}), a second DRG neuron was selected for its similar CIVDS response to the first one (Fig. 1 *B*). In Ca^{2+}-free solution, a step depolarization from −70 to 0 mV (200 ms) induced a rapid increase in C_m (ΔC_m) caused by CIVDS per se (Fig. 1 *B*, *left panel*, C_{m1}; also see Zhang and Zhou (18)). Subsequently, when the same cell was exposed to 2.5 mM Ca^{2+}, the same depolarization triggered Ca^{2+} influx via voltage-gated Ca^{2+} channels and a C_{m2} including both CIVDS and CDS (Fig. 1 *B*, *right panel*), comparable to the C_m(UV) in Fig. 1 *A* (*right*). Two phases of C_{m2} were noted: after an immediate rise, which reflected CIVDS as shown previously (18), there was a 0.5-s latency before a second and much slower increase occurred (Fig. 1 *B*, right; also see Zhang et al. (17)). This slow phase of C_{m2} was Ca^{2+}-dependent because removal of external Ca^{2+} completely eliminated the second phase but not the first phase. We subtracted C_{m1} from C_{m2} to reveal the pseudo-CDS component induced by depolarization (Fig. 1 *B*, *right*, $C_{m2} - C_{m1}$), which resemble the pure CDS induced by UV-flash (Fig. 1 *A*, *right*). Therefore, in a physiological solution containing 2.5 mM Ca^{2+}, depolarization-induced secretion (C_{m2}) included both components of CIVDS and CDS.

Increasing number of APs shifted secretion mode from CIVDS to combined CIVDS and CDS

Our next question was how CIVDS contributes to the total secretion under physiological stimuli. We used prerecorded real AP waveforms obtained from a current–clamp recording in a DRG neuron as stimulus templates and applied them to the soma of another DRG neuron under whole-cell voltage clamp according to the method described previously (32). Different AP patterns (or codes) were characterized by number and frequency. To test the effect of AP number on secretion, we first applied different numbers of APs at a fixed frequency of 20 Hz (32,35) to the somata of DRG neurons under voltage-clamp. The cells were dialyzed with fura-2K, a membrane-impermeable Ca^{2+} indicator, to measure intracellular Ca^{2+} concentration. Five APs at 20 Hz induced a significant increase in $[Ca^{2+}]_i$ in the presence of 2.5 mM extracellular Ca^{2+}, but no $[Ca^{2+}]_i$ change was detected in Ca^{2+}-free solution (Fig. 2 *A*, *left*, *lower panel*). Surprisingly, 5 APs generated similar ΔC_m, both in value and kinetics, in the presence or absence of extracellular Ca^{2+} (Fig. 2 *A*, *left*, *upper panel*). These data suggested that the $[Ca^{2+}]_i$ increase induced by low AP numbers failed to induce CDS. On the other hand, 20 APs at 20 Hz induced a larger $[Ca^{2+}]_i$ increase in 2.5 mM solution (Fig. 2 *A*, *right*, *lower panel*) and a twofold C_m increase over that in Ca^{2+}-free solution (Fig. 2 *A*, *right*, *upper panel*). This was consistent with the data shown in Fig. 1 *B*, both of which clearly showed a large CDS component under strong stimuli. The average ΔC_m triggered by 5 and 20 APs at 40 Hz in Ca^{2+}-free and 2.5 mM Ca^{2+} solution in the same neuron is shown in Fig. 2 *B*. Five, 20, and 40 APs were tested at 40 Hz, and the ratio of ΔC_m in Ca^{2+}-free to that in 2.5 mM Ca^{2+} indicated the fractional contribution of CIVDS to total secretion (Fig. 2, *C* and *D*). The fractional contribution of CIVDS to the total AP-induced secretion signal (C_m) was almost 100% when 5 APs were applied. The ratio decreased dramatically with increasing AP number from 5 to 40 (Fig. 2, *B* and *C*) at 40 Hz. These results indicated that small numbers of APs (weak stimulation) trigger CIVDS only, whereas large numbers of APs (strong stimulation), which resemble the conduction of pain signals (36,37), trigger both CIVDS and CDS. Furthermore, the increased CDS component under stronger stimuli was clearly caused by the increased $[Ca^{2+}]_i$.

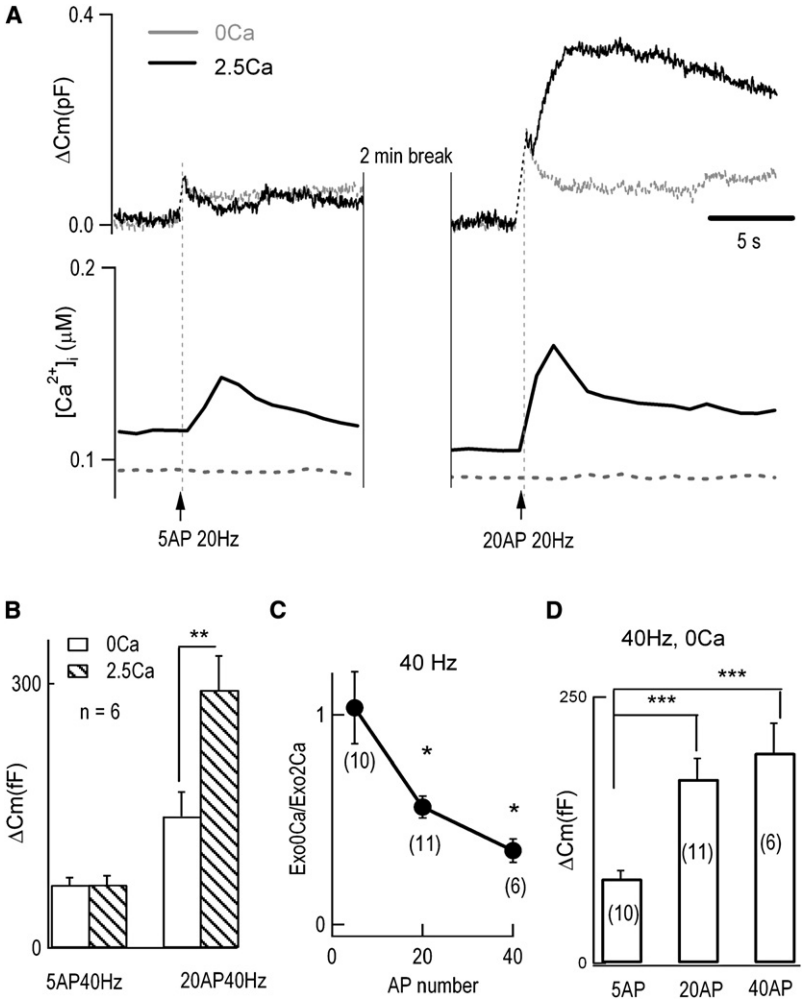

FIGURE 2 Larger AP number increases the fractional contribution by CDS. (*A*) Different AP numbers induced C_m signals (*upper panel*) in the presence (*solid traces*) or absence (*dashed traces*) of 2.5 mM Ca^{2+}. Simultaneous measurements of $[Ca^{2+}]i$ are also presented with 0.1 mM fura-2K in the patch pipette. The numbers of APs and their trigger times are shown. (*B*) Average results from six neurons; each neuron was stimulated by 5 APs at 40 Hz and 20 APs at 40 Hz in Ca^{2+}-free and 2.5 mM Ca^{2+} solutions. Empty bars represent Ca^{2+}-free bath, and striped bars represent the 2.5 mM Ca^{2+} condition. No significant difference was found when 5 APs at 40 Hz were applied ($\Delta C_m(0Ca) = 74 \pm 10$ fF; $\Delta C_m(2.5Ca) = 75 \pm 11$ fF); whereas a stronger stimulus, 20 APs at 40 Hz, induced a significant increase under 2.5 mM Ca^{2+} conditions ($\Delta C_m(0Ca) = 150 \pm 28$ fF; $\Delta C_m(2.5Ca) = 293 \pm 39$ fF; $p < 0.01$). (*C*) Fractional contribution of CIVDS to total AP-induced secretion in 2.5 mM Ca^{2+} extracellular solution. This was defined as the ratio of $\Delta C_m(0Ca)/\Delta C_m(2.5Ca)$. The fractional CIVDS induced by 5, 20, or 40 APs at 40 Hz were 1.03 ± 0.17, 0.56 ± 0.05, and 0.35 ± 0.06, respectively. For 5 APs vs. 20 APs: $p < 0.05$; 5 APs vs. 40 APs: $p < 0.01$; 20 APs vs. 40 APs: $p < 0.05$. (*D*) Average results of ΔC_m in Ca^{2+}-free bath triggered by 5, 20, or 40 APs at 40 Hz were 80 ± 8, 173 ± 19, and 198 ± 28 fF, respectively. Five APs at 40 Hz vs. 20 APs at 40 Hz: $p < 0.001$; 5 APs at 40 Hz vs. 40 APs at 40 Hz: $p < 0.001$; 20 APs at 40 Hz vs. 40 APs at 40 Hz: $p > 0.1$. Numbers in parentheses indicate number of cells.

Low AP frequency induced CIVDS alone, whereas high AP frequency also recruited the CDS component

In addition to AP number, the second parameter of an AP pattern, frequency, is known to regulate neurotransmitter release as well (3,25,32,38). Thus, we investigated whether different AP frequencies impacted the contribution of CIVDS and CDS to the soma secretion in DRG neurons.

When the number of APs was set at 5, either low frequency or high frequency induced similar C_m signals in the presence or absence of extracellular Ca^{2+} (data not shown). These results suggested that 5 APs at 40 Hz were not sufficient to induce CDS. When the number of APs was increased to 20, 1-Hz APs induced a similar C_m in the presence or absence of extracellular Ca^{2+}, suggesting that 20 APs at a low frequency still failed to accumulate sufficient intracellular Ca^{2+} for CDS. However, when 20 APs at 40 Hz were applied to the same cell, ΔC_m was dramatically increased in 2.5 mM Ca^{2+}, but not in Ca^{2+}-free solution (Fig. 3 *A*). The statistical results from 11 neurons showed that 20 APs at high frequency (40 Hz in Fig. 3 *B*; also see 20 Hz in Fig. 2 *A*) increased the CDS component by 94% ($p < 0.001$). In contrast, 20 APs at 1 Hz ($n = 4$) increased the CDS component by only 20% in the same neurons. Therefore, in DRG neurons, low-frequency stimuli ($\leq$4 Hz, probably mimicking spontaneous activity) mainly induced CIVDS, whereas high-frequency stimuli ($\geq$20 Hz, probably mimicking mechanical stimulation or pain) induced both CIVDS and CDS when AP numbers were large ($\geq$20). The CDS component increased with AP frequencies from 1 to 40 Hz (data not shown).

High AP frequency accelerated CIVDS-induced rapid endocytosis but not CDS-induced slow endocytosis

Following the two types of AP-induced exocytosis signals (CIVDS and CDS), there were also two types of exocytosis-coupled endocytosis signals, the fast endocytosis following CIVDS (Figs. 3 *A, right*, and 4 *A, left*), termed CIVDS-RE, and the slow endocytosis following CDS (Fig. 4 *A*, *right*), termed CDS-SE. Next, we investigated the effect of AP frequency on the two types of endocytosis signals. To define the effect of AP frequency on CIVDS-RE

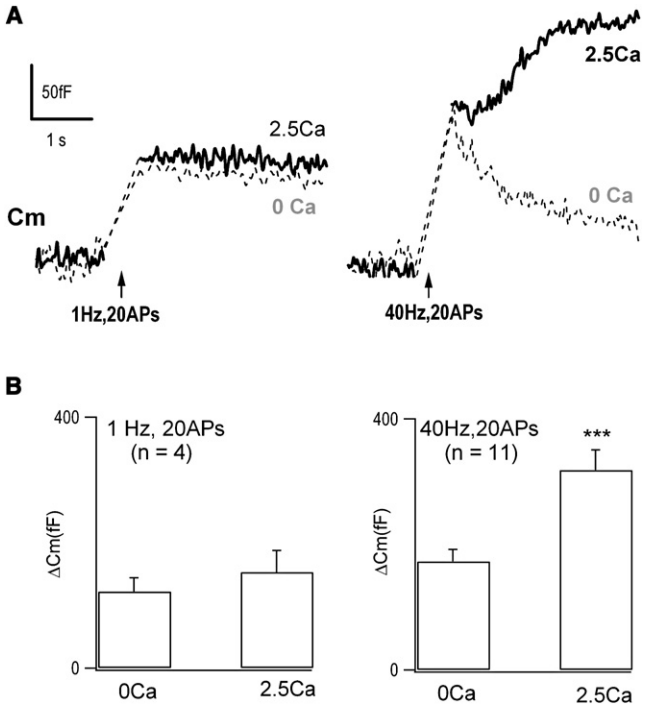

FIGURE 3 High AP frequency increases the CDS component in DRG neurons. (*A*) Profiles of ΔCm induced by different AP frequencies in the presence of 2.5 mM extracellular Ca^{2+} (solid traces) or in Ca^{2+}-free bath (*dashed traces*). (*B*) Averaged results showing that in Ca^{2+}-free bath, 20 APs at 1 Hz induced a similar secretion as in 2.5 mM Ca^{2+} (ΔC_m = 121 ± 22 fF; vs. 153 ± 35; $n = 4$). On the other hand, 20 APs at 40 Hz induced a greater secretion in 2.5 mM Ca^{2+} (ΔC_m = 318 ± 32 fF) than in Ca^{2+}-free solution (ΔC_m = 173 ± 19 fF, $p < 0.001$; $n = 11$).

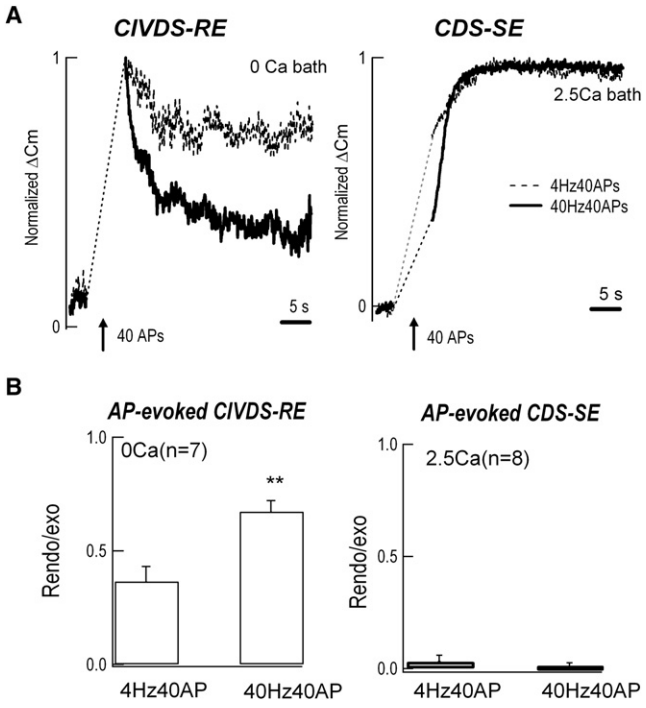

FIGURE 4 High AP frequency accelerates CIVDS-coupled rapid endocytosis (RE) but not CDS-coupled slow endocytosis (SE). (*A, left panel*) In Ca^{2+}-free extracellular solution, 40 APs at 40 Hz (*solid trace*) induced faster endocytosis than at 4 Hz (*dashed trace*). The C_m increases were 185 ± 21 fF and 122 ± 15 fF at 40 Hz and 4 Hz, respectively ($n = 7$). (*Right panel*) In 2.5 mM Ca^{2+}, 40 Hz or 4 Hz induced similar rates of endocytosis. The C_m increases were 551 ± 44 fF and 519 ± 58 fF at 40 Hz and 4 Hz, respectively ($n = 8$). (*B*) Averaged results showing the ratio of endocytosis to exocytosis at low and high frequencies. In the Ca^{2+}-free bath (*left panel*), the ratios at 4 Hz and 40 Hz were 0.37 ± 0.07 and 0.67 ± 0.05, respectively ($p < 0.001$, $n = 7$), whereas in 2.5 mM Ca^{2+} (*right panel*), the ratios were 0.03 ± 0.03 and 0.00 ± 0.02, without significant difference ($n = 8$).

and CDS-SE, the C_m ratio of total endocytosis in 30 s to maximum exocytosis ($R_{end/exo}$) in the absence or presence of extracellular Ca^{2+} was determined. To induce robust endocytosis, 40 APs at low (4 Hz) and high (40 Hz) frequencies were applied sequentially to a DRG neuron in Ca^{2+}-free solution (Fig. 4 *A*, *left*). The average data from seven independent experiments using 40 AP waveforms showed that the higher frequency accelerated CIVDS-RE (Fig. 4 *B*, *left*), consistent with our previous findings using 15 depolarization pulses (17). On the other hand, when 2.5 mM Ca^{2+} was puffed onto cells to assess the CDS-SE, the slow endocytosis induced by the different frequencies was similar (Fig. 4 *A*, *right*). The average CDS-SE from eight neurons showed no difference between 4 and 40 Hz (Fig. 4 *B*, *right*, $p > 0.05$). These data suggested that membrane retrieval following CIVDS and CDS are regulated differently and that, in contrast to CIVDS-RE, CDS-SE is independent of AP frequency. This finding in DRG somata differs from the CDS-SE in retinal bipolar cells and the calyx of Held (39,40).

Absence of CIVDS EPSCs in DRG terminals in the spinal cord

Finally, we investigated whether CIVDS also exists in DRG terminals. In primary cocultures of presynaptic DRG and postsynaptic DH neurons, EPSCs in DH neurons were evoked by applying 50 mM KCl to a nearby DRG neuron in the presence of 2.5 mM Ca^{2+} (Fig. 5). Removal of external Ca^{2+} completely blocked the evoked EPSCs, indicating the absence of CIVDS in cocultured DRG terminals (Fig. 5). In these cocultured neurons, as in the freshly isolated DRG neurons, depolarization induced both CIVDS (in Ca^{2+}-free bath) and CDS (in 2.5 mM Ca^{2+} bath) in the somata of DRG neurons (data not shown). In contrast, there was no depolarization-induced C_m increase in the soma of DH neurons (data not shown).

In freshly prepared spinal cord slices, presynaptic DRG terminal secretion generated EPSPs or EPSCs in postsynaptic DH neurons after field stimulation in the presence of 2.5 mM external Ca^{2+}. Both EPSCs and EPSPs were fully and reversibly blocked by removing external Ca^{2+} in the DRG-DH synaptic transmission (data not shown). Thus, evoked EPSCs/EPSPs at the DRG-DH synapses were fully Ca^{2+}-dependent. The transmitter that produces the EPSCs was glutamate (data not shown). However, these experiments did not exclude possible CIVDS-mediated synaptic release of a transmitter, which does not activate an ion channel.

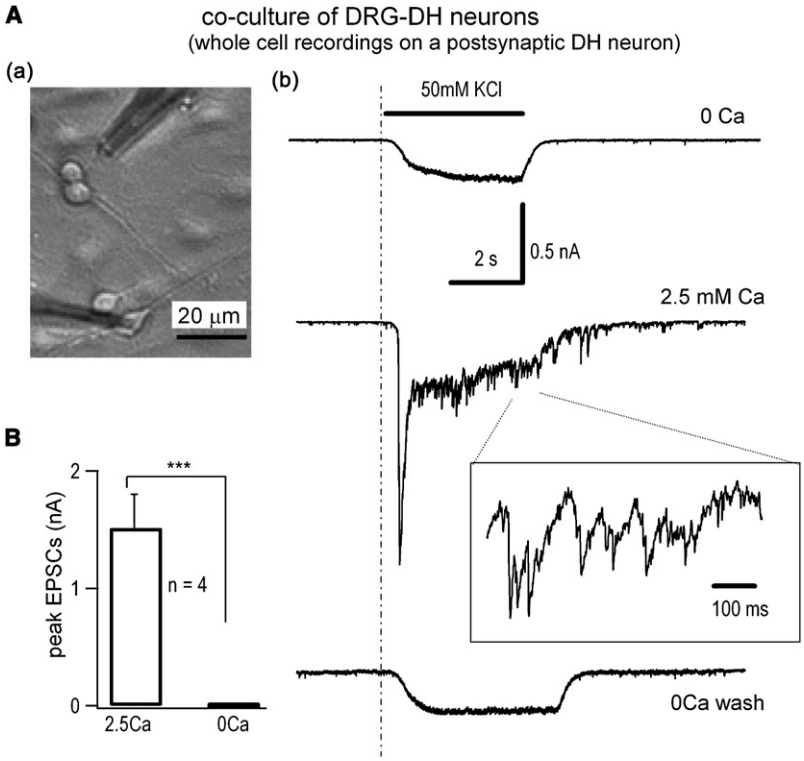

FIGURE 5 CIVDS does not contribute to EPSCs of DRG-DH synapses in primary cocultured DRG and DH neurons. (*A, upper left, a*) DRG and DH neurons were cocultured for at least 6 days before stimulation of DRG neurons with 50 mM KCl. (*Right, b*) Whole-cell EPSCs recorded in a DH neuron in Ca^{2+}-free and 2.5 mM Ca^{2+} bath solution. The bar represents the application of 50 mM KCl. Part of the EPSC trace at 2.5 mM Ca^{2+} was expanded. The slow changes in whole-cell currents during KCl application were probably caused by the voltage-independent K channels responsible for resting membrane potential. Similar results were obtained in four independent experiments. (*B*) Average results of the peak EPSCs, which were subtractions of total KCl-induced currents in 0 and 2.5 mM Ca^{2+} bath, from DRG-DH coculture was 1.5 ± 0.3 nA ($n = 4$).

DISCUSSION

In our previous study, we identified a unique form of secretion in the somata of DRG neurons, termed CIVDS (17,18). In this report, we applied capacitance measurements, UV-photolysis, whole-cell patch-clamp/intracellular recordings of EPSCs/EPSPs, and intracellular Ca^{2+} measurements to further define the characteristics of CIVDS and CDS in both somata and terminals of DRG neurons. Following physiological stimuli in the soma, both CIVDS and CDS were evoked, and their fractional contributions were modified by AP number and frequency. Exocytosis-coupled endocytosis was also modulated by the AP patterns. Finally, CIVDS occurred in the soma, but it does not contribute to EPSCs at the spinal synapses of DRG neurons.

Fractional contribution of CIVDS to total secretion depends on AP patterns

In the work presented here, we found that the relative contributions of CIVDS and CDS changed with AP number and frequency (Figs. 2 and 3). On one hand, AP-induced CDS depends on the size of the readily releasable vesicle pool (RRP) and its refilling rate after vesicle depletion (41). On the other hand, CDS is also sensitive to how $[Ca^{2+}]_i$ is increased, i.e., by Ca^{2+} influx from voltage-gated Ca^{2+} channels or release from intracellular Ca^{2+} stores (42,43). In DRG neurons, the RRP sizes for CIVDS and CDS are ~200 and 1000 fF (18), corresponding to 400 and 2000 dense-core vesicles (assuming 140 nm diameter for both types of vesicles) (44), respectively, and the half-refilling time of the CIVDS RRP is 0.75 s (18). In this work, the strongest AP stimulus (40 APs at 40 Hz) released nearly all of the RRP of CIVDS but only a small fraction of the RRP for CDS (Fig. 4). Because the size of the CDS RRP was not the limiting factor in our experiments, AP-induced CDS mainly depended on the increase of $[Ca^{2+}]_i$. According to the $[Ca^{2+}]_i$ measurements, low AP number and frequency failed to accumulate sufficient intracellular Ca^{2+} for CDS (3,32,45). Thus, low AP number and frequency induced only CIVDS, whereas high AP number and frequency increased the CDS component by increasing $[Ca^{2+}]_i$ above the threshold required for triggering CDS.

AP frequency-dependent modulation is different for CDS and CIVDS

AP-induced exocytosis is coupled with endocytosis for membrane retrieval. Here, we demonstrated that the two exocytosis-endocytosis pairs of CIVDS and CDS were both sensitive to the AP frequency. In the CIVDS exocytosis-endocytosis pair, AP frequency positively modulated the endocytosis (RE) but not the exocytosis (CIVDS), resulting a *positive* modulation of CIVDS endocytosis/exocytosis ratio by AP frequency (Figs. 3 and 4) (17). In the CDS exocytosis-endocytosis pair, AP frequency positively modulated the exocytosis (CDS) but not the endocytosis (SE), resulting a *negative* modulation of CDS endocytosis/exocytosis ratio by AP frequency (Figs. 3 and 4).

Relation between CIVDS and CDS in a DRG soma

To establish the relation between CIVDS and CDS vesicle pools, we induced pure CIVDS, CDS, and both together in the same neurons. Pure CDS was obtained by UV-flash-induced rises in $[Ca^{2+}]_i$. Pure CIVDS was induced by depolarization in a Ca^{2+}-free solution. Both CIVDS and CDS, distinguished by their kinetics, were induced at the same time by depolarization in 2.5 mM Ca^{2+}, and the Ca^{2+}-dependent component (CDS) was obtained by subtracting CIVDS from the total secretion ($C_{m2} - C_{m1}$) in a neuron (Fig. 1). Thus, the depolarization-induced secretion consisted of both CDS and CIVDS in the soma at physiological levels of stimulation. This permitted us to determine the fractional contributions by CIVDS and CDS in response to different AP patterns. Note that, in addition to ''pure'' CDS and ''pure'' CIVDS components, it is not clear whether C_{m2} contains a third component, which depends on both Ca^{2+} and voltage per se.

Absence of CIVDS-induced EPSCs in DRG spinal terminals

Soon after the finding of CIVDS in the somata of DRG neurons (17,18), Erwin Neher's group reported that CIVDS does not occur in the giant synapse of the calyx of Held (46). DRG neurons form presynaptic terminals that synapse with dorsal horn neurons in the spinal cord. In the work presented here, we determined whether DRG neurons express CIVDS in their spinal terminals as they do in the soma. According to the experiments using three independent protocols (patch-clamp recording of EPSCs in cocultures of DRG and DH neurons, patch-clamp recording of EPSCs in spinal DRG-DH slices, and extracellular field potential recordings of EPSPs in spinal DRG-DH slices), all presynaptic membrane depolarization-induced EPSCs are Ca^{2+}-dependent in DRG-DH synapses (Fig. 5). These experiments exclude CIVDS-induced postsynaptic currents in the DRG terminals. However, it could not exclude CIVDS-releasing ligand(s), which bind metabolic receptors (i.e., CGRPs). Future work should determine whether CIVDS neuromodulators exist in DRG terminals.

Physiological relevance of CIVDS

DRG neurons are primary afferent neurons that convey somatosensory information to the spinal cord and brain. Nociceptive signals are conducted mainly by small DRG neurons ($<30\ \mu m$), which were used in our studies. In these neurons, APs induce transmitter release at both nerve terminals (Fig. 5) and the soma (7,18,37). High-frequency (~40 Hz) AP patterns resulting from nociceptor activation in vivo (36,47) induce marked somatic release, which may lead to sympathetic nerve spouting around DRG neurons and satellite cell activity (48,49). The 40-Hz AP pattern used in our study mimics painful stimuli (37). Our data showed that the number and frequency of APs impacted the contributions of the CIVDS and CDS components in secretion. Some C-neurons in DRG exhibit spontaneous activity, which is 1 Hz or less. During those spontaneous activities, compared to CDS, CIVDS should play major role in soma release. When the number and frequency were high (≥ 20 Hz), which might mimic APs during physiological or pathological pain, CDS contributed more than CIVDS in the soma. Therefore, CIVDS may be the main form of somatic secretion under normal resting conditions in DRG neurons.

The study presented here using capacitance measurements has several limitations. First, it is not clear which transmitters, such as CGRP, SP, ATP, or/and others, were released by CIVDS and CDS. Second, the fractional contributions of CIVDS versus CDS were determined by C_m measurements, which may not be proportional to the amount of neurotransmitter released (50). Nevertheless, this work addresses one physiologically relevant aspect of CIVDS and CDS during DRG somatic secretion. AP patterns regulate the two types of exocytosis and their coupled endocytosis in the somata of DRG neurons. Because pain-related neurotransmitters (such as CGRP, SP, and ATP) are released from DRG somata following membrane depolarization (7,18,26,27), these special features may play important roles in physiology and pathology of mammalian primary sensation and pain.

We thank Dr. Iain C. Bruce for comments on the manuscript.

This work was supported by grants from the National Basic Research Program of China (2006CB500800 and G2007CB512100) and the National Natural Science Foundation of China (30728009, 30770788 and 30770521), and a ''985'' grant from the Chinese Department of Education.

REFERENCES

1. Zucker, R. S. 1996. Exocytosis: a molecular and physiological perspective. *Neuron.* 17:1049–1055.
2. Augustine, G. J., M. P. Charlton, and S. J. Smith. 1987. Calcium action in synaptic transmitter release. *Annu. Rev. Neurosci.* 10:633–693.
3. Zhou, Z., and S. Misler. 1995. Action potential-induced quantal secretion of catecholamines from rat adrenal chromaffin cells. *J. Biol. Chem.* 270:3498–3505.
4. Neher, E., and R. S. Zucker. 1993. Multiple calcium-dependent processes related to secretion in bovine chromaffin cells. *Neuron.* 10:21–30.
5. Shahrezaei, V., A. Cao, and K. R. Delaney. 2006. Ca^{2+} from one or two channels controls fusion of a single vesicle at the frog neuromuscular junction. *J. Neurosci.* 26:13240–13249.
6. Sudhof, T. C. 2004. The synaptic vesicle cycle. *Annu. Rev. Neurosci.* 27:509–547.
7. Huang, L. Y., and E. Neher. 1996. Ca^{2+}-dependent exocytosis in the somata of dorsal root ganglion neurons. *Neuron.* 17:135–145.
8. Cohen, R., and D. Atlas. 2004. R-type voltage-gated Ca^{2+} channel interacts with synaptic proteins and recruits synaptotagmin to the plasma membrane of *Xenopus* oocytes. *Neuroscience.* 128:831–841.
9. Wiser, O., M. K. Bennett, and D. Atlas. 1996. Functional interaction of syntaxin and SNAP-25 with voltage-sensitive L- and N-type Ca^{2+} channels. *EMBO J.* 15:4100–4110.

10. Wiser, O., M. Trus, A. Hernandez, E. Renstrom, S. Barg, et al. 1999. The voltage sensitive Lc-type Ca^{2+} channel is functionally coupled to the exocytotic machinery. *Proc. Natl. Acad. Sci. USA.* 96:248–253.

11. Sheng, Z. H., J. Rettig, M. Takahashi, and W. A. Catterall. 1994. Identification of a syntaxin-binding site on N-type calcium channels. *Neuron.* 13:1303–1313.

12. Mochida, S., Z. H. Sheng, C. Baker, H. Kobayashi, and W. A. Catterall. 1996. Inhibition of neurotransmission by peptides containing the synaptic protein interaction site of N-type Ca^{2+} channels. *Neuron.* 17:781–788.

13. Rettig, J., C. Heinemann, U. Ashery, Z. H. Sheng, C. T. Yokoyama, et al. 1997. Alteration of Ca^{2+} dependence of neurotransmitter release by disruption of Ca^{2+} channel/syntaxin interaction. *J. Neurosci.* 17:6647–6656.

14. Bezprozvanny, I., P. Zhong, R. H. Scheller, and R. W. Tsien. 2000. Molecular determinants of the functional interaction between syntaxin and N-type Ca^{2+} channel gating. *Proc. Natl. Acad. Sci. USA.* 97:13943–13948.

15. Parnas, H., J. C. Valle-Lisboa, and L. A. Segel. 2002. Can the Ca^{2+} hypothesis and the Ca^{2+}-voltage hypothesis for neurotransmitter release be reconciled? *Proc. Natl. Acad. Sci. USA.* 99:17149–17154.

16. Singer-Lahat, D., A. Sheinin, D. Chikvashvili, S. Tsuk, D. Greitzer, et al. 2007. K^+ channel facilitation of exocytosis by dynamic interaction with syntaxin. *J. Neurosci.* 27:1651–1658.

17. Zhang, C., W. Xiong, H. Zheng, L. Wang, B. Lu, et al. 2004. Calcium- and dynamin-independent endocytosis in dorsal root ganglion neurons. *Neuron.* 42:225–236.

18. Zhang, C., and Z. Zhou. 2002. Ca^{2+} -independent but voltage-dependent secretion in mammalian dorsal root ganglion neurons. *Nat. Neurosci.* 5:425–430.

19. Yang, H., C. Zhang, H. Zheng, W. Xiong, Z. Zhou, et al. 2005. A simulation study on the Ca^{2+}-independent but voltage-dependent exocytosis and endocytosis in dorsal root ganglion neurons. *Eur. Biophys. J.* 34:1007–1016.

20. Chen, X., L. Wang, Y. Zhou, L. H. Zheng, and Z. Zhou. 2005. "Kiss-and-run" glutamate secretion in cultured and freshly isolated rat hippocampal astrocytes. *J. Neurosci.* 25:9236–9243.

21. Wightman, R. M., J. A. Jankowski, R. T. Kennedy, K. T. Kawagoe, T. J. Schroeder, et al. 1991. Temporally resolved catecholamine spikes correspond to single vesicle release from individual chromaffin cells. *Proc. Natl. Acad. Sci. USA.* 88:10754–10758.

22. Chen, X. K., L. C. Wang, Y. Zhou, Q. Cai, M. Prakriya, et al. 2005. Activation of GPCRs modulates quantal size in chromaffin cells through G($\beta\gamma$) and PKC. *Nat. Neurosci.* 8:1160–1168.

23. Bruns, D., and R. Jahn. 1995. Real-time measurement of transmitter release from single synaptic vesicles. *Nature.* 377:62–65.

24. Jaffe, E. H. 1998. Ca^{2+} dependency of serotonin and dopamine release from CNS slices of chronically isolated rats. *Psychopharmacology (Berl.).* 139:255–260.

25. Huang, H. P., S. R. Wang, W. Yao, C. Zhang, Y. Zhou, et al. 2007. Long latency of evoked quantal transmitter release from somata of locus coeruleus neurons in rat pontine slices. *Proc. Natl. Acad. Sci. USA.* 104:1401–1406.

26. Bao, L., S. X. Jin, C. Zhang, L. H. Wang, Z. Z. Xu, et al. 2003. Activation of δ opioid receptors induces receptor insertion and neuropeptide secretion. *Neuron.* 37:121–133.

27. Zhang, X., Y. Chen, C. Wang, and L. Y. Huang. 2007. Neuronal somatic ATP release triggers neuron-satellite glial cell communication in dorsal root ganglia. *Proc. Natl. Acad. Sci. USA.* 104:9864–9869.

28. Gu, J. G., and A. B. MacDermott. 1997. Activation of ATP P2X receptors elicits glutamate release from sensory neuron synapses. *Nature.* 389:749–753.

29. Nakatsuka, T., and J. G. Gu. 2001. ATP P2X receptor-mediated enhancement of glutamate release and evoked EPSCs in dorsal horn neurons of the rat spinal cord. *J. Neurosci.* 21:6522–6531.

30. Lao, L. J., Y. Kawasaki, K. Yang, T. Fujita, and E. Kumamoto. 2004. Modulation by adenosine of Aδ and C primary-afferent glutamatergic transmission in adult rat substantia gelatinosa neurons. *Neuroscience.* 125:221–231.

31. Wu, B., Y. M. Wang, W. Xiong, L. H. Zheng, C. L. Fu, et al. 2005. Optimization of a multi-channel puffer system for rapid delivery of solutions during patch-clamp experiments. *Front. Biosci.* 10:761–767.

32. Duan, K., X. Yu, C. Zhang, and Z. Zhou. 2003. Control of secretion by temporal patterns of action potentials in adrenal chromaffin cells. *J. Neurosci.* 23:11235–11243.

33. Heinemann, C., R. H. Chow, E. Neher, and R. S. Zucker. 1994. Kinetics of the secretory response in bovine chromaffin cells following flash photolysis of caged Ca^{2+}. *Biophys. J.* 67:2546–2557.

34. Xu, T., B. Rammner, M. Margittai, A. R. Artalejo, E. Neher, et al. 1999. Inhibition of SNARE complex assembly differentially affects kinetic components of exocytosis. *Cell.* 99:713–722.

35. Abdulla, F. A., and P. A. Smith. 2001. Axotomy- and autotomy-induced changes in the excitability of rat dorsal root ganglion neurons. *J. Neurophysiol.* 85:630–643.

36. Fang, X., S. McMullan, S. N. Lawson, and L. Djouhri. 2005. Electrophysiological differences between nociceptive and non-nociceptive dorsal root ganglion neurones in the rat in vivo. *J. Physiol.* 565:927–943.

37. Zhang, X. F., C. Z. Zhu, R. Thimmapaya, W. S. Choi, P. Honore, et al. 2004. Differential action potentials and firing patterns in injured and uninjured small dorsal root ganglion neurons after nerve injury. *Brain Res.* 1009:147–158.

38. Elhamdani, A., Z. Zhou, and C. R. Artalejo. 1998. Timing of dense-core vesicle exocytosis depends on the facilitation L-type Ca channel in adrenal chromaffin cells. *J. Neurosci.* 18:6230–6240.

39. Sun, J. Y., X. S. Wu, and L. G. Wu. 2002. Single and multiple vesicle fusion induce different rates of endocytosis at a central synapse. *Nature.* 417:555–559.

40. von Gersdorff, H., and G. Matthews. 1994. Inhibition of endocytosis by elevated internal calcium in a synaptic terminal. *Nature.* 370:652–655.

41. Gillis, K. D., R. Mossner, and E. Neher. 1996. Protein kinase C enhances exocytosis from chromaffin cells by increasing the size of the readily releasable pool of secretory granules. *Neuron.* 16:1209–1220.

42. von Ruden, L., and E. Neher. 1993. A Ca-dependent early step in the release of catecholamines from adrenal chromaffin cells. *Science.* 262:1061–1065.

43. Augustine, G. J., and E. Neher. 1992. Calcium requirements for secretion in bovine chromaffin cells. *J. Physiol.* 450:247–271.

44. Zhang, X., K. Aman, and T. Hokfelt. 1995. Secretory pathways of neuropeptides in rat lumbar dorsal root ganglion neurons and effects of peripheral axotomy. *J. Comp. Neurol.* 352:481–500.

45. Klingauf, J., and E. Neher. 1997. Modeling buffered Ca^{2+} diffusion near the membrane: implications for secretion in neuroendocrine cells. *Biophys. J.* 72:674–690.

46. Felmy, F., E. Neher, and R. Schneggenburger. 2003. The timing of phasic transmitter release is Ca^{2+}-dependent and lacks a direct influence of presynaptic membrane potential. *Proc. Natl. Acad. Sci. USA.* 100:15200–15205.

47. Xu, G. Y., L. Y. Huang, and Z. Q. Zhao. 2000. Activation of silent mechanoreceptive cat C and Aδ sensory neurons and their substance P expression following peripheral inflammation. *J. Physiol.* 528:339–348.

48. Xie, W. R., H. Deng, H. Li, T. L. Bowen, J. A. Strong, et al. 2006. Robust increase of cutaneous sensitivity, cytokine production and sympathetic sprouting in rats with localized inflammatory irritation of the spinal ganglia. *Neuroscience.* 142:809–822.

49. Zhang, J. M., H. Li, and M. A. Munir. 2004. Decreasing sympathetic sprouting in pathologic sensory ganglia: a new mechanism for treating neuropathic pain using lidocaine. *Pain.* 109:143–149.

50. Neher, E. 1998. Vesicle pools and Ca^{2+} microdomains: new tools for understanding their roles in neurotransmitter release. *Neuron.* 20:389–399.